Remarks on Signal Processing in HF Radars Using FMCW Modulation

Klaus-Werner Gurgel
University of Hamburg
Institute of Oceanography
Bundesstrasse 53
D-20146 Hamburg, Germany
Email: gurgel@ifm.uni-hamburg.de
Tel: +49-40-42838-5742
Fax: +49-40-42838-5713

Thomas Schlick
University of Hamburg
Institute of Oceanography
Bundesstrasse 53
D-20146 Hamburg, Germany
Email: thomas.schlick@zmaw.de
Tel: +49-40-42838-5746
Fax: +49-40-42838-5713

***Abstract*—Besides the well known microwave radar systems mainly used in navigation, surveillance, and control applications, High-Frequency (HF) radars gain increased attention during the last decades. These HF radars are operated in the 3-30 MHz frequency range and due to ground-wave or sky-wave propagation provide over-the-horizon (OTH) capabilities. Many of these OTH radars apply frequency modulated continuous wave (FMCW) modulation for range resolution, which enables them to operate with a relatively low transmit power of a few watts only. Sometimes these types of radars are referred to as "silent radar". This paper discusses the signal processing chain from deramping the received signal down to processing of range-Doppler-azimuth spectra. Some steps which are critical for the overall system performance are discussed in detail and a new technique to derive the structure of radio frequency interference (RFI), which is superposed to the radar echoes, is described.**

I. Introduction

High-Frequency (HF) radars gain increased attention during the last decades. Because HF radars are operated in the 3-30 MHz frequency range, they can make use of ground-wave or sky-wave propagation. High working ranges can be achieved enabling the detection of targets or the measurement of ocean surface parameters like wave spectra or near-surface currents at ranges far behind the horizon. Because of their over-the-horizon (OTH) capabilities, HF radars are also referred to as OTH radars. Besides echoes from ships or other targets, there is a strong backscatter signal due to the roughness of the ocean surface (Crombie 1955 [2]). The process causing these echoes is Bragg-resonant scattering from ocean waves of half the electromagneic wavelength. As these ocean waves travel at a well defined phase speed, they generate distinct peaks in the backscatter Doppler spectrum. The peaks and the sidebandes around them can be exploited to measure maps of ocean currents (Barrick 1977 [1]), sea state, and wind. However, these strong backscatter signals provide problems to the target detection capabilities. A thresholding technique has been published by Dzvonkovskaya [3] in 2008 to reduce the number of false alarms due to ocean clutter in HF radars.

Many of the OTH radars are based on frequency modulated continuous wave (FMCW) modulation to provide range resolution. This technique enables them to operate with a relatively low transmit power of a few watts only ("silent radar"). A paper on FMCW modulation and it's compatibility with other radio services has been published by Gurgel and Schlick [7]. In 1996, the WERA (WEllen RAdar) HF radar for applications in oceanography has been developed at the University of Hamburg (Gurgel *et al*. 1998 [5]), which implements FMCW modulation based on Direct Digital Synthesizers (DDS).

Section II gives a short description of the FMCW principle and discusses the influence of different windowing functions which must be applied prior to the range-resolving FFTs.

Section III describes the dynamic range requirements in a FMCW based HF radar. Besides the strong signal received from the transmit antenna on the direct path - the radar transmits and receives simultaneously - the weak echoes from far ranges must be processed. A high dynamic range of the analog and digital receiver stages is needed. In a coherent system, a significant processing gain due to temporal integration helps to implement the dynamic range requirements.

Section IV discusses a new technique to derive the pattern of radio frequency interference (RFI), which is only avaliable in case of FMCW modulation and an I/Q demodulator for de-ramping.

Section V describes WERA's digital beam forming technique, which simultaneously provides multible beams to all requested directions from $-60°$ to $+60°$ without any mechanical movement or switching. In addition, an increase of the signal-to-noise ratio of 12 dB can be achieved for specific directions when combining the signals of 16 independent antennas.

II. FMCW Radar De-Ramping and Windowing Functions

A FMCW radar transmits a linear frequency chirp covering a bandwidth B within the chirp duration T. The bandwidth is directly related to the range resolution, e.g. a bandwith $B = 100$ kHz gives 1.5 km range resolution. The depth of a range cell is $r = \frac{c}{2B}$, with c beeing the speed of light. Fig. 1 shows the principle of FMCW modulation as it has been implemented with the WERA HF radar (Gurgel *et al*.

1998 [5]). For a given range, an echo of the transmitted chirp is received at some time delay τ. By mixing the received signal with the transmitted chirp, the echo is de-ramped and the time delay τ is transformed to a constant frequency offset Δf, cf. Gurgel and Schlick [7].

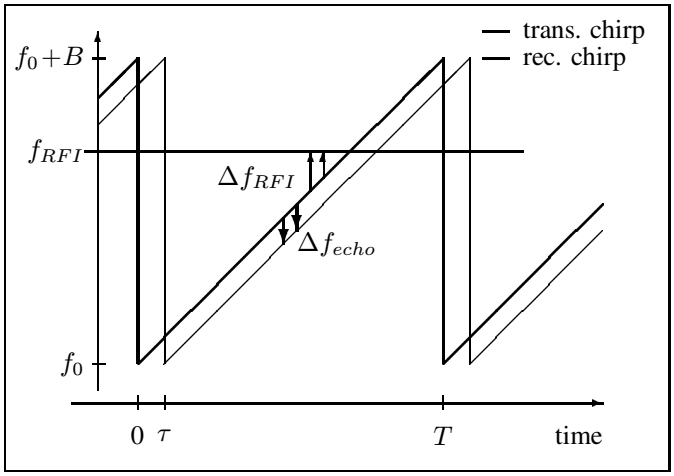

Fig. 1. The process of de-ramping the received radar echo using the transmitted chirp. For a given range, the frequency offset Δf_{echo} is a constant negative value. The chirp passes the operating frequency f_{RFI} of an assumed radio service.

Note, that in case of a chirp with an increasing frequency (positive chirp), this frequency shift is always negative, while chirps with a decreasing frequency (negative chirp) result in positive frequency offsets. An I/Q demodulator for de-ramping can split positive and negative frequency offsets and in this way avoid aliasing the noise from the "unused side" of the spectrum, gaining 3 dB in signal-to-noise ratio. The transmitted frequency chirp $s(t)$ is given by

$$s(t) = A_s\, cos\, \varphi_s = A_s\, cos(2\pi(f_0 + \frac{B}{2T}\, t)\, t + \phi_{s0}) \qquad (1)$$

with A_s being the Amplitude and ϕ_{s0} the starting phase of the chirp. The actual frequency of the transmitted chirp ω_s is

$$\omega_s = \frac{d\varphi_s}{dt} = 2\pi(f_0 + \frac{B}{T}t) \qquad (2)$$

The received signal $r(t)$ at a time delay τ is described by

$$r(t) = A_r\, cos\, \varphi_r = A_r\, cos(2\pi(f_0 + \frac{B}{2T}\,(t-\tau))\,(t-\tau) + \phi_{s0}) \qquad (3)$$

with A_r being the Amplitude and ϕ_{s0} the starting phase. The actual frequency of the received echo ω_r is

$$\omega_r = \frac{d\varphi_r}{dt} = 2\pi(f_0 + \frac{B}{T}t - \frac{B}{T}\tau) \qquad (4)$$

The I/Q demodulator consists of two mixers to generate the in-phase (I) and quadrature-phase (Q) components by multipying the received signal $r(t)$ with the transmitted chirp, $A_s\, cos\, \varphi_s$ and $A_s\, sin\, \varphi_s$ respectively:

$$I(t) = \frac{A_r A_s}{2}(cos(\varphi_r - \varphi_s) + cos(\varphi_r + \varphi_s)) \qquad (5)$$

$$Q(t) = \frac{A_r A_s}{2}(sin(\varphi_r - \varphi_s) + sin(\varphi_r + \varphi_s)) \qquad (6)$$

The component $(\varphi_r + \varphi_s)$ at the output of the I/Q demodulator is suppressed by a low pass filter or just omitted in case of a numerical simulation. The remaining part of the in-phase signal is

$$I(t) = \frac{A_r A_s}{2} cos(2\pi(\frac{B}{2T}\tau^2 - f_0\tau - \frac{B}{T}\tau t)) \qquad (7)$$

Differentiating gives the actual frequency ω_I

$$\omega_I = -2\pi\frac{B}{T}\tau \qquad (8)$$

Similar calculations can be done for the quadrature-phase signal. The resulting I and Q components are digitized and passed to a complex FFT.

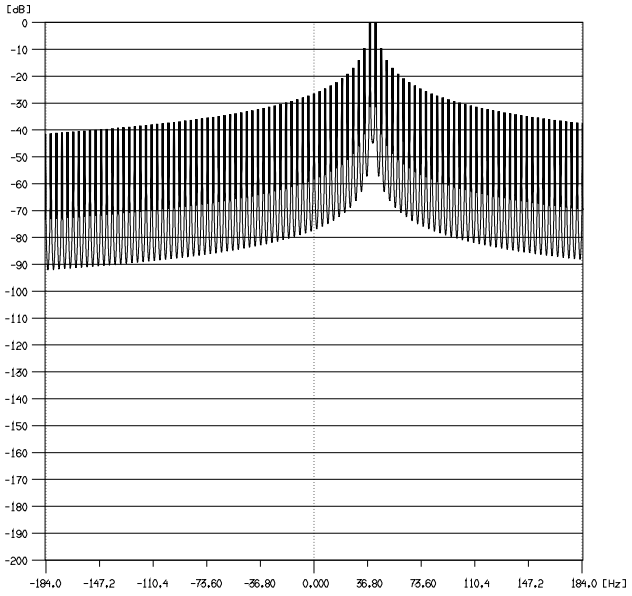

Fig. 2. Range smearing due to phase inconsistancies between end and start of a chirp. The energy of the simulated echo, located between range cells 10 and 11, is strongly smeared to neighbouring range cells.

Within the WERA system, a typical chirp duration is $T = 0.26$ seconds. The de-ramped chirp is sampled 1536 times, which relates to a sample rate of about 6 kHz. The complex FFT of the sampled signal provides spectral lines at $1/T = 3.846$ Hz spacing, which represent the range cells in frequency domain. In case of a positive chirp, the spectral lines from DC to increasing negative frequencies give one sample of the received signal for increasing range cells numbers. This is the FFT providing range resolution of the radar. By processing a sequence of coherent frequency chirps and forming a time series of the sampled signal within the range cells, the phase variation can be tracked and the Doppler spectra within each range cell can be processed.

There is one problem related to this approach, which must be taken into accout: At the start of each chirp, there is a short

time, when the de-ramping mixer produces a huge frequency offset $B - \Delta f$. This signal is always present and the strongest one is received from the direct path to the transmit antenna. It is generated by the "fly-back" of the chirp and introduces a strong pulse, which hides the coherence of the signal for a short time. Fig. 2 shows the result of a numerical simulation based on a sequence of 128 chirps at $f_0 = 12.0$ MHz start frequency, $B = 125$ kHz bandwidth and $T = 0.26$ seconds duration, which results in a frequency offset of 3.846 Hz between range cells. A modulation due to assumed ocean waves to simulate the first-order Bragg lines has been added at ± 1.0 Hz. The time delay τ of the echo was adjusted to be located in the centre between range cell 10 and 11. It can be seen that the power of this echo is not only distributed to range cells 10 and 11, but it is strongly smeared to neighbouring range cells, masking echoes at these range cells.

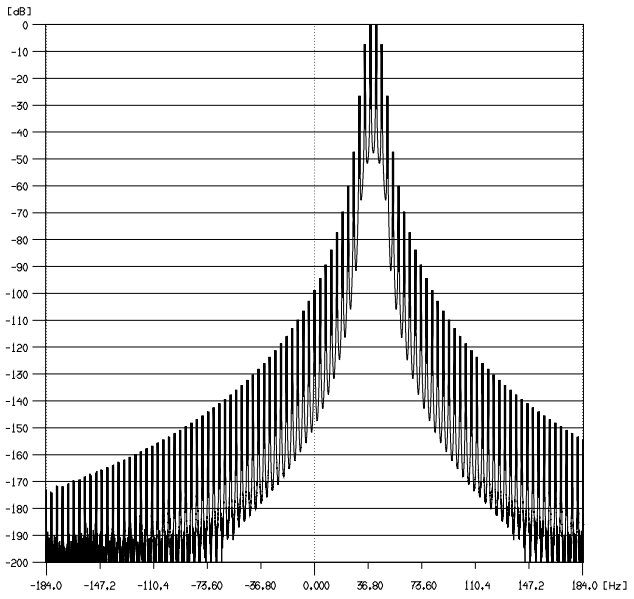

Fig. 3. After applying a $\cos^4$ windowing function to each chirp before applying the range-resolving FFT, the energy of the simulated echo smeared to neighbouring range cells is significantly reduced.

This "fly-back" problem can be solved by applying a windowing function to the samples of each chirp, before calculating the range resolving FFT. Good candidates for this windowing are a Blackman-Harris window and a $\cos^4$ function (shown in Fig. 3). The smeared energy in the directly adjacent range cells (number 9 and 12) is slightly increased, but all other range cells receive significantly less smeared energy, providing nearly undistorted echoes for farer ranges.

III. FMCW Radar Dynamic Range

Dynamic range is a critical issue in FMCW radar systems. As transmitter and receiver are operated simultaneously, the strong signal received from the transmit antenna on the direct path as well as weak echoes from far ranges must be processed together. In contrast to pulsed systems, increasing the receiver gain with range is no option.

To achieve a high dynamic range, it is important that the amplifier and mixer stages must be selected for high intercept point values. A/D conversion and FFT processing must also be designed carefully. In case of the WERA system, the dynamic range is as follows: The A/D converter (ADC) provides 16 bit resolution, which gives 96 dB dynamic range. An ADC with a high Spurious Free Dynamic Range (SFDR) is required here. The range resolving FFT is based on 1536 samples, which gives 31.75 dB. The Doppler resolving FFT increases the Signal to Noise Ratio (SNR) by 27 dB in case of 512 samples. In this example, the coherent integration time is 133.12 seconds and a total dynamic range of 154.75 dB can be achieved in theory.

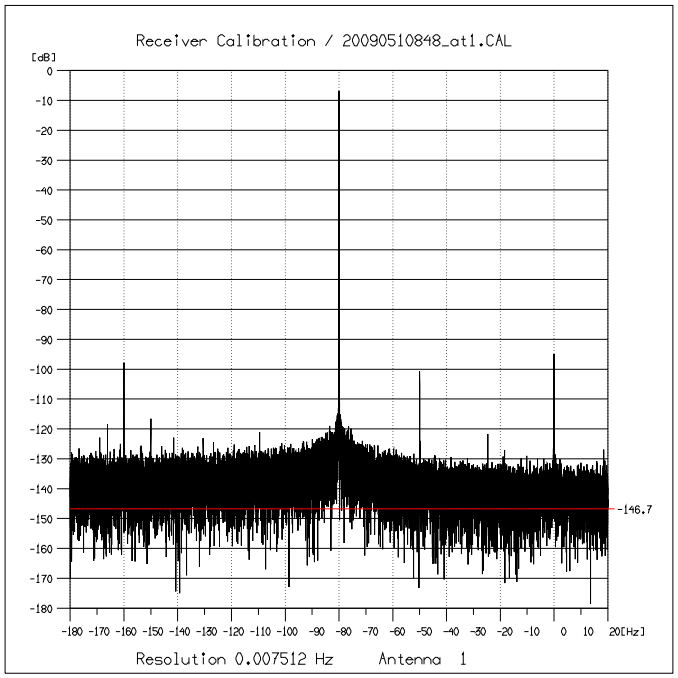

Fig. 4. The dynamic range of the WERA HF radar. A calibration signal of -38 dBm at -80 Hz frequency offset is shown. The noise level is at -146.7 dB.

Fig. 4 shows the result of a calibration test at the conditions mentioned above. 0 dB is related to a receiver input power of -32 dBm. The frequency offset between transmitter and receiver is set to -80 Hz. Other signals can be seen at DC, -50 Hz (line power frequency), -150 Hz (second harmonic of line power frequency), and -160 Hz (first harmonic of -80 Hz). The noise level is found at -146.7 dB. This value is higher than the theorectical value for the dynamic range, because the noise generated inside the amplifiers is designed to be slightly above the noise level due to quantization.

As the transmit power is $+45$ dBm, an isolation of 32 dB + 45 dB = 77 dB is required between transmitter and receiver. This is achieved by 3 steps: a) putting a minimum of the transmitter's antenna gain diagram towards the receive antennas, b) providing enough spacing between the receive and

transmit antennas, and c) installing a high-pass filter behind the de-ramping mixer to slightly attenuate the echoes from the first range cells. It shall also be noted, that the sideband noise introduced by the master clock of the system is a critical parameter in high dynamic range FMCW configurations.

IV. FMCW Radar RFI Processing

HF radars have to share the radio frequencies with other radio services. Due to the daily ionospheric cycle, the electromagnetic environment is highly variable. Gurgel and Barbin [8] (2008) describe a 4-step method to minimize the impact or Radio Frequency Interference (RFI). This paper gives an update to the method of RFI compensation using the structure of the RFI. This technique can be applied in case of FMCW modulation and if an I/Q demodulator is used for de-ramping.

As mentioned in section II, frequency chirps to higher frequencies always result in the echoes to appear on the negative side of the spectrum ("signal side"). The positive side of the spectrum contains noise only. If the radar chirps over the frequency used by a radio service, the de-ramped signal contains a solitary pulse from positive frequencies to Dc and then to negative frequencies (cf. Fig. 1). This pulse generates a specific structure in the range-Doppler spectra calculated from the radar echoes. However, the "noise side" of the de-ramped signal shows a structure quite similar to "signal side", except that there are no echoes. The signals from the "noise side" of the de-ramped signal can then be used to describe the structure of the RFI on the "signal side".

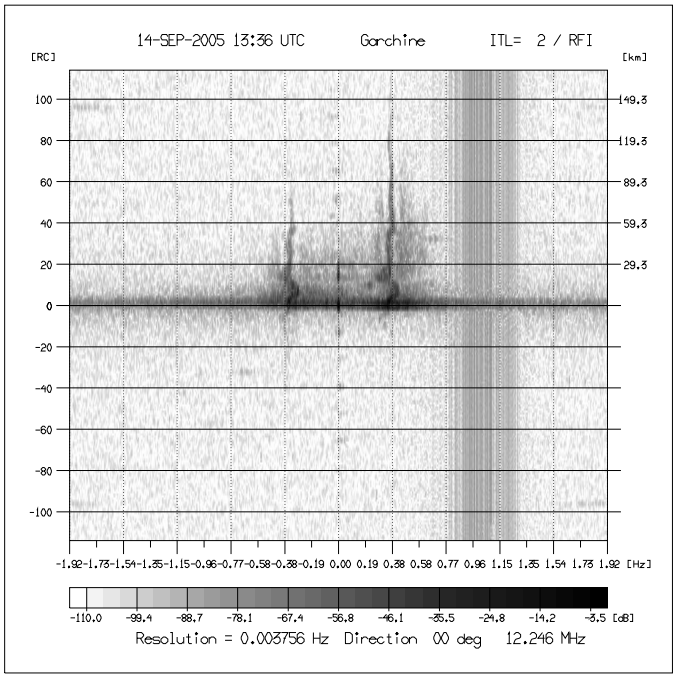

Fig. 5. A range-Doppler spectrum measured at 18-Aug-2005. Positive Range Cells (RC) show radar echoes, while the negative range cells shows radio frequency interference only.

Fig. 5 shows an example of a range-Doppler spectrum measured during an experiment in France near Brest. The radar center frequency was set to 12.253 MHz, the bandwidth to 100 kHz (1.5 km range resolution). The upper part of the figure shows the spectrum of radar echoes vs. range and RFI at Doppler frequencies around 1.2 Hz. The lower part of the figure shows the spectra acquired at the "noise side", noted by negative range cell numbers, which contains RFI only. The RFI generates vertical lines in the range-Doppler spectrum, covering both signal and noise sides. To reduce the impact of RFI on the radar measurements, the "noise side of" the range-Doppler spectrum can be "subtracted" from the signal side using a special filter technique, which improves the data quality in 60 % to 80 % of the RFI cases.

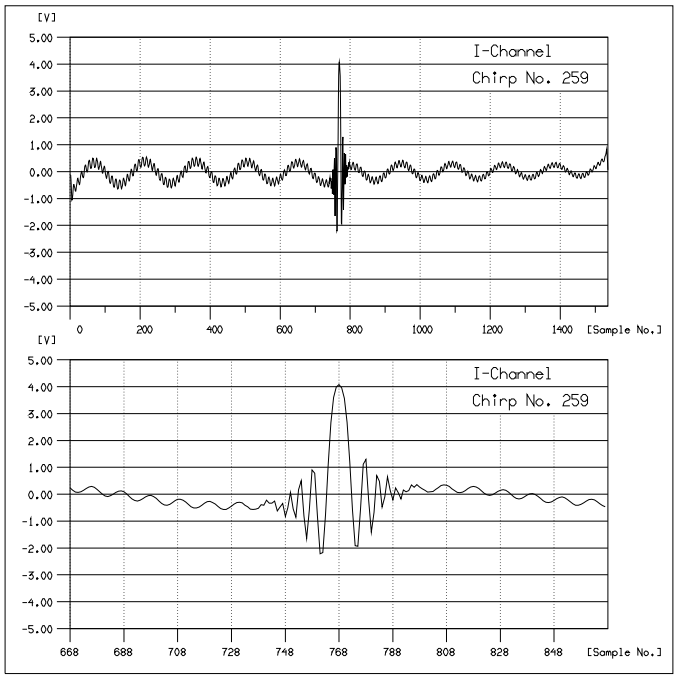

Fig. 6. The I channel of a simulated chirp after de-ramping and filtering. The solitone generated while passing an RFI signal with a constant frequency can be seen at sample number 768. The other signals are due to synthesized echoes at range cells 10.5 and 140.

The numerical simulation has been extended to include the direct path signal, modulated echoes from two different ranges, and one RFI signal. The frequency chirp from 12.0 MHz to 12.125 MHz is synthesized by simulating the DDS phase accumulator at a DDS master clock of 45.37 MHz. The received signal is generated by shifting the synthesized chirp in time for each echo and modulating it with Doppler frequencies. The direct path signal is located at 500 m range. All these are summed up and finally a constant frequency RFI at 12.0625 MHz + 1.0 Hz is added. This simulated received signal is then de-ramped with the transmitted chirp. A digital filter is used to implement the analog high-pass and low-pass filter characteristics of the system. At the end, the signal is re-sampled to generate data which are compatible to the system's data structure and can be processed by using standard software.

Fig. 6 shows the time series of a selected chirp. The solitone generated by passing over the RFI signal can clearly be seen.

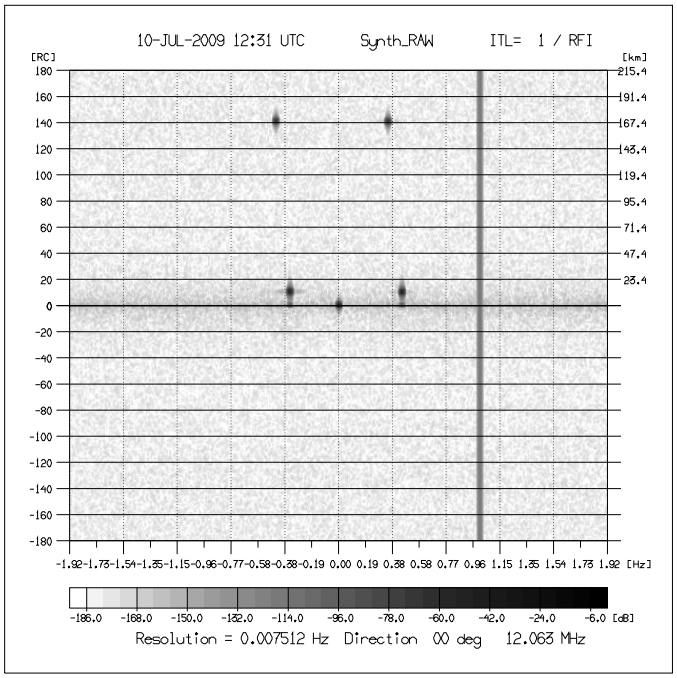

Fig. 7. The range-Doppler spectrum of the simulated signal (see text).

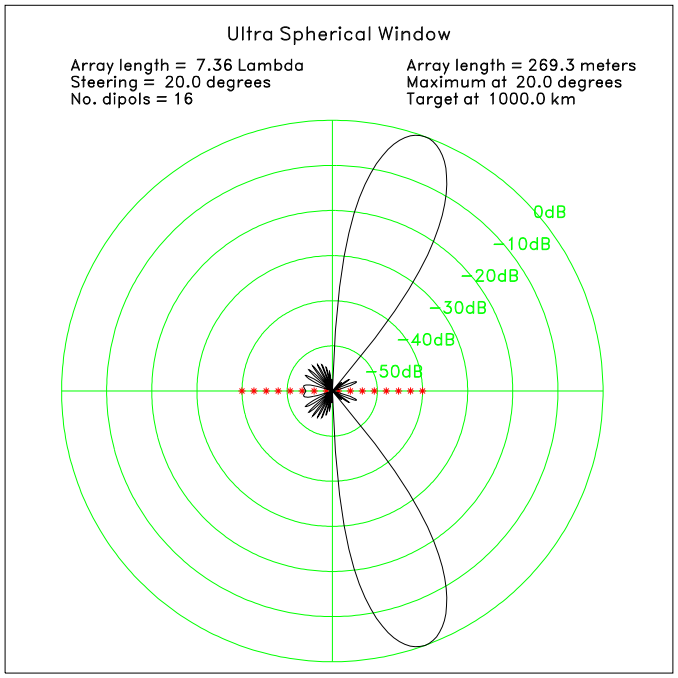

Fig. 8. The antenna pattern of a beam formed to 20 degrees based on 16 antennas installed along a straight line.

Also, the echoes from range cell 10.5 (low frequency component) and 140 (high frequency component) can be identified. Fig. 7 shows the range-Doppler spectrum calculated from 512 chirps. The RFI signal is mapped to +1.0 Hz Doppler shift. Frequency offsets from the center frequency are aliased back into the range-Doppler spectra frequency range by multiples of $1/T$. Slowly changing RFI frequencies make a band of vertical lines.

V. HF Radar Beam Forming

WERA applies a parallel approach for the receive channels. There are 16 antennas connected to 16 independent receivers. Adding up the signals from 16 antennas provides an increase of the signal-to-noise ratio by 12 dB. Amplitudes and phases of the receiver channels including the antenna cables are calibrated. This is essential for a good suppression of side lobes. To adopt the antenna calibration to a changing environment, the energy around the first-order Bragg lines received by each antenna is used for on-line normalization.

To avoid phase ambiguities, the antenna spacing should be less than 0.5 λ, where λ is the electromagnetic wave length. Simulations show that a good value for the antenna spacing is 0.45 λ (cf. Fig. 8). To suppress side lobes, a windowing function has to be applied before shifting the phases and summing up the signals to steer the beam to the requested direction. The phases are calculated from the distance of each single antenna in the array to the location the beam should point to in World Geodetic System (WGS84) coordinates. This way, curved arrays or random spaced antennas can also be handled by the beam forming algorithm. The most practical way in a craggy landscape is to install the antennas at possible locations and to measure their locations by differential GPS.

Conclusion

Important processing steps to sucessfully operate a FMCW radar in the HF frequency band have been discussed. This includes the selection of windowing functions, requirements on dynamic range and direct path suppression, special handling of times, where radio frequency interference may degrade the system performance, and digital beam forming implemented in software, which provides simultaneous access to all beam directions. These processing steps define nowaday's state-of-the-art of advanced HF radar technology. They have been developed and implemented when designing the WERA HF radar at the University of Hamburg.

References

[1] D.E. Barrick, M.W. Evans, B.L. Weber, *Ocean surface current mapped by radar* Science 198, pp. 138-144, 1977.

[2] D.D. Crombie, *Doppler spectrum of sea echo at 13.56 Mc/s* Nature, vol. 175, pp. 681-682, 1955.

[3] A.L. Dzvonkovskaya, K.-W. Gurgel, H. Rohling, T. Schlick, *Low Power High Frequency Surface Wave Radar Application for Ship Detection and Tracking* Radar 2008 Conference, Adelaide, Australia, Proceedings, 2008.

[4] K.-W. Gurgel and G. Antonischki, *Remote Sensing of Surface Currents and Waves by the HF Radar WERA* Seventh IEE Conference on Electronic Engineering in Oceanography, Proceedings, pp. 211-217, 1997.

[5] K.-W. Gurgel, G. Antonischki, H.-H. Essen, T. Schlick, *Wellen Radar (WERA), a new ground-wave based radar for ocean remote sensing*, Coastal Engineering, 37, pp. 219-234, 1999.

[6] K.-W. Gurgel, Y. Barbin, T. Schlick, *Radio Frequency Interference Suppression Techniques in FMCW Modulated HF Radars*, IEEE Oceans 2007 Europe, proceedings, Jun. 2007.

[7] K.-W. Gurgel and T. Schlick, *Compatibility of FMCW Modulated HF Surface Wave Radars with Radio Services*, International Radar Symposium IRS 2007, Cologne, Germany, proceedings, pp. 255-258, Sept. 2007.

[8] K.-W. Gurgel and Y. Barbin, *Suppressing Radio Frequency Interference in HF Radars*, Sea Technology, Compass Publications, www.sea-technology.com, pp. 39-42, March 2008.